Powder agglomeration patterns at acoustic driving observed by sonoluminescence technique

O. A. Korotchenkov[a] and T. Goto
Department of Physics, Graduate School of Science, Tohoku University, Sendai 980-8578, Japan

(Received 2 February 1998; accepted for publication 5 October 1998)

A sonoluminescence (SL) technique gives a sensitive probe to detect spatial agglomeration patterns produced in powder mixtures subjected to acoustically driven plate. Studies of the surface-integrated SL intensity with increasing driving amplitude yield data about variations of the packing density on the surface of vibrating powders. Imaging of spatial distributions of the SL intensity enables direct measurement of the size of agglomeration patterns. The size of the patterns is found to be $\sim 10^2$ μm in a 3-μm-sized powder at a driving frequency of about 4 MHz. The distribution of the average sonoluminescence intensity across the pattern is attributed to the density gradient while rapid variations in the SL intensity across the pattern are suggested to give the particle velocity distribution within the pattern. The temporal changes of the SL intensity can be used to study time evolutions of dense powder arrangements. © *1999 American Institute of Physics.* [S0021-8979(99)01302-X]

I. INTRODUCTION

It is well known that granular materials exhibit many unusual properties.[1] In particular, vibrating powders produce convection, segregation, and agglomeration behaviors[1–5] resembling those found in fluids, so that the analogy between powder and fluid dynamics are often used.[6] On the basis of this analogy, qualitative explanations of vibration-induced flow and mixing of granular materials have been put forward.[6–8] However, dynamics of a steady state in the system subjected to vibrations are quite complex, and, in many cases, the underlying physical mechanisms are still somewhat uncertain.

On the other hand, the motivation for studying particle agglomeration phenomena lies in their applications in industrial processes such as mechanical processing in pharmacology, building materials, industrial handling and drying, processing of composite materials, pipeline transfer of solids, etc. In spite of increased interest, experimental techniques which provide a detection of particle rolls are rather limited although important insights have been obtained with x-ray and neutron scattering techniques,[9,10] magnetic resonance,[11,12] and capacitance[13] imagings, tracking of particle motions on a video tape or a charge coupled device (CCD) camera.[4,14]

The sonoluminescence (SL) effect in granular medium[15] offers a promising tool for visualization of powder compaction phenomena. There are also indications that this effect can be used for imaging of a wide range of impacts between particles because of collision-induced origin of SL. Given that powder grinding, shaking, and milling usually involve the full range of frictional interactions between colliding particles, powder examination by the sonoluminescence technique is of interest.

In this article, we document our studies of powder agglomeration dynamics captured by the sonoluminescence technique. Agglomeration patterns arise in powder subjected to acoustic driving. We find that, with the approach we have taken, one can learn much there is to know about such important quantities as powder packing densities, gradients in dense packing arrangements, and time evolutions of particle packing. Since we only imaged the illuminating surface, it is inconceivable that subsurface powder patterns may be involved. Therefore, our present work leaves open the question of how much one can infer from surface measurements about the details of particle packing structures beneath the surface, if any.

II. EXPERIMENTAL PROCEDURE

A mixture of 99.999% purity ZnS:Mn (0.5 wt %) grains of different sizes and slightly anisotropic shapes was obtained from the Furuuchi Chemical Company. The size of the particles was measured optically. The shape distribution of powder grains was characterized by a ratio d_1/d_2 of the maximum to the minimum linear dimension of the grain (inset of Fig. 1). This distribution taken for $N_0=200$ particles is shown in Fig. 1. The average grain diameter of particles with $d_1 \approx d_2$ was roughly 3 μm.

A powder was contained in a 6 mm diameter and about 1 mm depth cylindrical glass-walled flask and closed with two plates, as shown in Fig. 2. The bottom plate was made of glass, and the cover plate was made of $LiNbO_3$. Acoustic driving was provided by a 500-μm-thick Y- or 41°Y-cut $LiNbO_3$ piezoelectric cap, a 1-mm-wide gold electrode, and a semitransparent ground plane made of gold, as shown in Fig. 2. Application of a radio-frequency (rf) voltage U to the electrode generated Z-propagating plate acoustic waves in $LiNbO_3$ occurs with a mixture of vertical and horizontal displacements at the surfaces of the plate.[16] We could launch plate waves at frequencies ranging from 1 to 6 MHz. The

[a]Permanent address: Faculty of Physics, Kiev University, Kiev 252022, Ukraine; electronic mail: olegk@tower.ups.kiev.ua

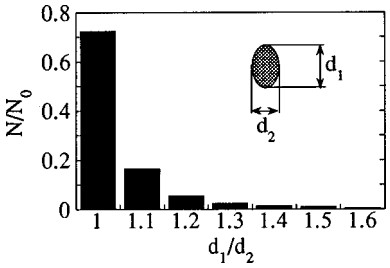

FIG. 1. A shape distribution histogram of powder particles characterized by a ratio (d_1/d_2).

frequency was then tuned in order to achieve the maximum sonoluminescence intensity, so that the data presented below were taken at ≈4.2 MHz which is close to the frequency of a lowest thickness eigenmode of the plate.

The SL experiments used powders of different starting packing densities of grains (''more packed'' powder and ''less packed'' powder). To prepare a more packed mixture, the flask was slightly overloaded with a powder and then pressed downward by a cover plate. For a less packed starting powder, the excess of the grains in the overloaded flask was removed before covering the container by a cover plate. We define the packing density η of a powder to be the mass of a powder divided by the calculated mass of ZnS in the volume of the container. For less packed initial conditions, we found $\eta_l^0 = 0.37$. When a powder was prepared in a more packed initial state, the packing density was close to $\eta_m^0 = 0.39$. Because of the initial compression of the powder by a cover plate, a filled volume fraction was likely underestimated near the powder surface, particularly, in a more packed powder. Hence, reported η^0 is not exactly equivalent to the packing density of a powder near the driving plate. Although the contribution of the powder surface cannot be determined with high precision, we believe that η_l^0 is very close to the true surface value while η_m^0 is probably within a factor of 1.2 of the true value.

The luminescence light transmitted by a transparent $LiNbO_3$ plate was imaged onto a two dimensional 576 ×384 CCD camera (Princeton Instruments) with low-aberrating optics. The system was found to be linear over the SL signal variation range. A 1 mm area of the sample surface was imaged by roughly 330 pixels of the CCD camera such that the resulting geometric resolution of about 3 μm was close to the average size of the grains. The actual spatial resolution was somewhat larger mainly because of the roughness of an illuminating surface.

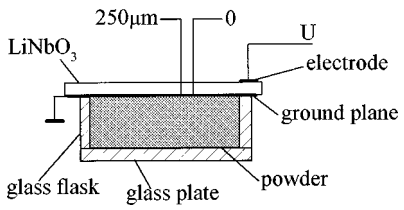

FIG. 2. Schematic of the side view of the ultrasonic cell, indicating the approximate location of powder patterns (labels 0 and 250 μm) from where the SL cross sections were taken. A cylindrical glass flask, and glass and $LiNbO_3$ plates confine a powder material. An acoustic driving is achieved by applying a rf voltage U to a metal electrode.

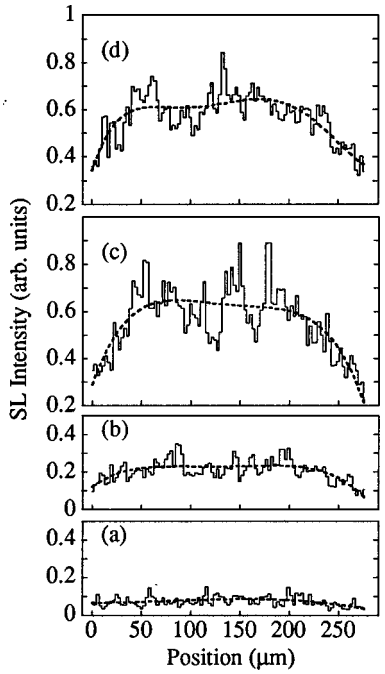

FIG. 3. Evolution of the SL intensity cross section with the driving amplitude increasing from (a) to (d) at a given location on the illuminating surface (0 through 250 μm in Fig. 2) taken in a more packed powder. Panels (a), (b), (c), and (d) are taken at the driving voltages denoted, respectively, by arrows *a*, *b*, *c*, and *d* in Fig. 5(b) for closed circles. Dashed lines are smooth fits to the data points that are proposed to describe the density gradients within the illuminating pattern. The light emission is acquired over 1 s well after the drive is on.

A photomultiplier tube (Hamamatsu Photonics R106) followed by a picoammetr TR8641 and a servocorder SR6211 was accomplished to examine the temporal behavior of sonoluminescence. These measurements were limited to at least one second in their time resolution. All experiments presented here were performed at room temperature.

III. RESULTS AND DISCUSSION

We were able to observe sonoluminescence in a ZnS:Mn powder for driving voltages U above the luminescence threshold. An illuminating surface was characterized by spatially distributed luminescence spots that were imaged to produce two-dimensional snapshots of the surface color.[15] The surface color is a measure of the interparticle interactions, and this is a prerequisite for studying the dynamics of powder particles. In this way, the driven-induced evolution of powder arrangements could be serially monitored by imaging the evolution of arbitrary cross sections through the interior of a powder pattern.

The imaged SL cross sections along the sound wave axis between locations indicated in Fig. 2 are exhibited in Figs. 3 and 4. They reveal that the SL intensity is roughly uniform at low driving amplitudes [in Figs. 3(a) and 4(a)] while inhomogeneous illuminating patterns are visible at higher driving [in Figs. 3(b)–3(d) and 4(b)–4(d)]. Similar patterns have been observed at other locations on the illuminating surface. Evidently, the patterns of enhanced emissions are present

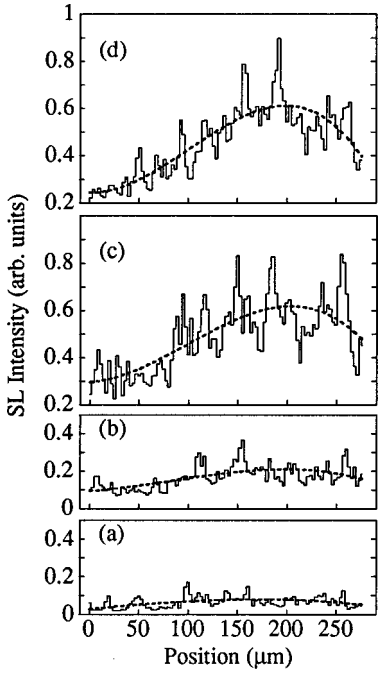

FIG. 4. Same evolution as Fig. 3, but with a powder prepared in a less packed initial conditions. Panels (a), (b), (c), and (d) are taken at the driving voltages denoted, respectively, by arrows *a*, *b*, *c*, and *d* in Fig. 5(b) for open circles.

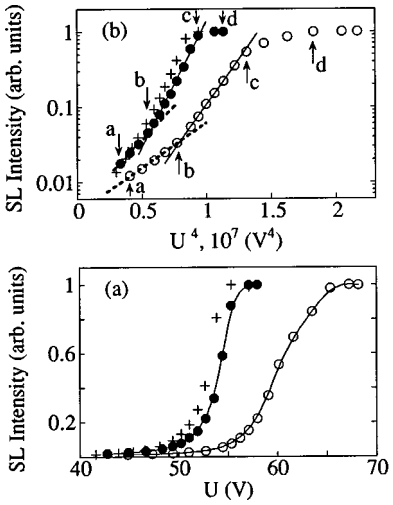

FIG. 5. Panel (a) displays the dependence of the total image computed SL intensity on the driving voltage U in less packed (open circles) and more packed (closed circles) powders. Crosses illustrate the departure from closed circles taken after five sweeping runs of the driving. The dependencies are normalized to their maximum value. The lines are guides to the eye. In panel (b) the logarithm of the SL intensity is shown as a function of U^4 for the data presented in panel (a). Solid and dashed lines in (b) indicate fits to Eq. (2) using circle data points which they intersect. The SL images were acquired from a 6-mm-diam area of the powder during 1 s well after the imposed driving.

that are extended through 100–200 μm ($\sim$30–70 particle diameters) on the powder surface. It has been suggested already previously that the enhanced emissions come from the regions of increased packing densities of grains.[15]

As a test of this suggestion, a few distinct experiments have been performed starting from less packed and more packed initial conditions. Figure 5(a) shows the surface-integrated SL intensity as a function of U, using less packed (open circles) and more packed (closed circles) starting powders. These data are taken in freshly packed mixtures. For comparison, we show as crosses the data taken in a more packed powder after five sweeping runs of U, i.e., after successively reducing the driving voltage to zero and then returning it back to a maximum value. These results demonstrate that the surface-integrated intensity of SL depends rather sensitively on the packing density of a powder [open and closed circles in Fig. 5(a)], and that the packing fraction itself seems to depend on the driving [closed circles and crosses in Fig. 5(a)].

There is currently no accurate method to calculate the SL intensity in powders, so an approximate model was constructed.[15] In this model, the occurrence of SL is treated in the framework of a simplified molecular kinetic approach for particle motions driven by a $LiNbO_3$ plate such that the intensity I of SL is presumed to be related to the average velocity v of a powder particle near the driving plate and the average spacing ξ between nearest grains

$$\ln I \propto (2\sigma)^2 \rho^2 v^4 / \xi^2, \tag{1}$$

where σ is the radius of particles which are assumed to be identical and spherical, $\rho \propto m/(2\sigma)^3$ is the particle density, and m is the mass of the particle. In the context of the above equation, the threshold of SL exhibited in Fig. 5(a) is related to a threshold velocity v that a particle acquires during its collision with the driving plate. Although the distribution of particle velocities is expected to be broad, SL is likely generated only by rapid particles the number of which is greater the larger the driving voltage. As a very rough guess for the choice of an appropriate value of v in Eq. (1), we reduce the first estimate to $v \propto fA \propto fU$, where A is the amplitude of the vibrating surface and f is the driving frequency. Therefore, v is assumed to be proportional to the driving plate velocity, fA, at the collision point, so we write

$$\ln I \propto (2\sigma)^2 \rho^2 f^4 U^4 / \xi^2. \tag{2}$$

With these assumptions, we examine the dependence of $\ln I$ on U^4; see Fig. 5(b). The luminescence intensity goes primarily as the fourth power of the driving voltage U, so in the figure we include dashed-line fits to Eq. (2). At higher driving, as already assumed above, the intergrain separation ξ is expected to decrease within agglomeration patterns, and this requires that the slope of the fit to Eq. (2) should increase. That is what we see in Fig. 5(b): In the regions marked ''*ab*'' and ''*bc*'' open circles indeed can be fit by two straight lines such that a slope of the solid-line fit is substantially greater than that of the dashed-line fit. The existence of such a distinctive break point b for open circles appears to be a fairly convincing evidence that the SL enhancement above this point is predominantly caused by an increased packing density in a less packed powder. In contrast, the dashed- and solid-line fits to closed circles in Fig. 5(b) are not nearly as reliable as that for open circles because the regions *ab* and *bc* are not quite straight for closed circles and the break point b cannot be accurately fixed. Therefore, increased packing densities on the powder surface would

presumably be partly responsible for what we believe to be enhanced emissions taken in a more packed powder above point b in Fig. 5(b) determined by eye.

It is worth noting in this respect that Eq. (1) is based on a simple caricature of the effects accompanying an oscillating driving by incorporating both the theoretical pressure on grains and the experimental emission intensity as a function of applied pressure.[15] We therefore believe that the physics we have included in our model is sufficiently complete to roughly describe dynamics of grain particles undergoing SL. However, this approach is nontrivial to accurately implement various components which might govern the occurrence of SL such as driven-induced particle alignment effects together with a space distribution of the emission from a grain, heating of grain surfaces by the driving, etc. In this context, more detailed work is needed for collectively accounting for many features of the SL effect in powders.

If we assume that the physics that governs the observed emission can be approximated by Eq. (1) so that the enhanced emitted light with increasing the driving is due to increasing particle velocities [in the regions *ac* in Fig. 5(b)] and decreased interparticle spacings in agglomerated patterns (above points b), then the simplification introduced allows the packing densities of powder particles near the driving plate to be computed entirely from the data in Fig. 5(b). What is required is a concomitant measurement of a starting packing density η^0 in either powder. We take $\eta_l^0=0.37$ for a less packed powder (dashed-line fit to open circles) as if the grains were spherical with $\sigma=1.5$ μm. Assuming $(4/3)\pi(\sigma+\xi/2)^3$ to be the volume per grain in a mixture, we write the packing density

$$\eta=\sigma^3/(\sigma+\xi/2)^3. \tag{3}$$

With these assumptions, the intergrain spacings ξ are computed from Eq. (2) and from these the SL-measured packing densities $\eta_{(\mathrm{SL})}$ for the dashed- and solid-line fits in Fig. 5(b). We find $\xi_l^0=1.18$ μm (dashed-line fit to open circles), $\xi_l=0.83$ μm and $\eta_{(\mathrm{SL})l}=0.48$ (solid-line fit to open circles), $\xi_m^0=0.96$ μm and $\eta_{(\mathrm{SL})m}^0=0.43$ (dashed-line fit to closed circles), $\xi_m=0.71$ μm and $\eta_{(\mathrm{SL})m}=0.53$ (solid-line fit to closed circles). It is seen that the slopes of the fits to closed circles, respectively, in the regions *ab* and *bc* are greater than those to open circles. This is apparently prescribed by Eq. (2), as long as the packing in a less packed powder is looser and the spacing ξ is greater compared to that in a more packed powder.

The data on SL-measured packing densities obtained at low driving amplitudes are then to be compared with the values of η derived from the mass of a powder contained in the flask (see Sec. II). The results of such a comparison are shown in Fig. 6. They reveal that η values calculated from the mass of a powder are smaller than $\eta_{(\mathrm{SL})}$ values computed from Eqs. (2) and (3). Thus, matching the $\eta_{(\mathrm{SL})}$ and η values in a less packed powder we find the SL-measured packing density in a more packed powder $\eta_{(\mathrm{SL})}=\eta_{(\mathrm{SL})m}^0=0.43$ whereas the value obtained from a powder mass, $\eta=\eta_m^0=0.39$, is substantially smaller. The above argument suggests that η gives the average volume packing density whereas $\eta_{(\mathrm{SL})}$ is related to the surface packing density.

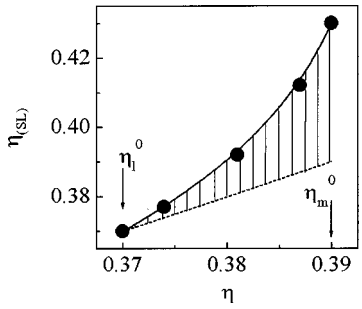

FIG. 6. SL-measured packing density $\eta_{(\mathrm{SL})}$ vs η determined from a powder mass. The values $\eta_{(\mathrm{SL})}$ and η are matched at $\eta=\eta_l^0=0.37$. Arrows η_l^0 and η_m^0 indicate packing densities of starting powders used in this work. Solid line is a guide to the eye, dotted line indicates $\eta_{(\mathrm{SL})}=\eta$. Hatched area shows the difference $\eta_{(\mathrm{SL})}-\eta$.

Therefore, with the method of powder compaction used in our experiments, surface area contributing to SL would tend to give the higher values of $\eta_{(\mathrm{SL})}-\eta$ the greater the value of η. This is confirmed by the experiments; see Fig. 6. Hence we conclude that SL measurements likely provide more accurate values of a packing density in the surface area regions of initially compressed powders compared to averaged values obtained by measurements of a powder mass.

In order to gain a deeper insight, we will first compare the data of Fig. 5(b) with that of Figs. 3 and 4. It is seen that the average SL intensity exhibited by dashed curves in Figs. 3 and 4 shows rapid increase across the illuminating pattern in a more packed powder in panels (b) and (c) of Fig. 3, i.e., in the region *bc* for closed circles in Fig. 5(b). This is opposed to more gradual increase in the average SL intensity across the pattern in a less packed powder [panels (b) and (c) in Fig. 4]. Increasing *U* above points *c* in Fig. 5(b), the light intensity eventually saturates, roughly in agreement with the absence of significant changes from panels (c) to panels (d) in Figs. 3 and 4. Therefore, there are qualitative similarities between the trends of the surface-integrated SL intensity (Fig. 5) and its distribution across the illuminating pattern (Figs. 3 and 4). We interpret these observations as indicating that the data on the surface-integrated luminescence intensity shown in Fig. 5 purport to determine the densities of powder packing given above.

Another feature of the data exhibited in Figs. 3 and 4 that has direct bearing on powder packing is the occurrence of rapid variations in the SL intensity across the illuminating patterns. These variations achieve the greatest values in panels (c) of Figs. 3 and 4. In fact, they are substantially suppressed in a more packed powder at higher driving [panel (d) in Fig. 3] although the variations remain significant in a less packed powder [panel (d) in Fig. 4]. The consequence is that the saturation of the SL intensity exhibited above points c in Fig. 5(b) appears to be more gradual in a less packed powder (open circles) compared to that in a more packed powder (closed circles). We conjecture that the distribution of the average SL intensity across the illuminating patterns (dashed curves in Figs. 3 and 4) gives the density gradients within the patterns while the rapid variations in the SL intensity bear directly on the particle velocity distributions. It is therefore implied that the dashed curves in Figs. 3 and 4 represent

concentration profiles and the solid curves resemble velocity profiles of powder particles averaged over image acquisition time.

These proposed conjectures are supported by a number of observations. First, the presence of agglomeration patterns leads to an appreciable reduction in grain velocities v thus eventually decreasing SL intensities with increasing the driving voltage U [Eq. (1)] and explaining the saturation of the dependencies exhibited in Fig. 5(b) above points c. Furthermore, the proposed interpretation naturally explains greater suppression of the SL intensity variations observed at a high driving in a more packed powder [panel (d) in Fig. 3] compared to that in a less packed powder [panel (d) in Fig. 4]. This can be attributed to reduced velocities of powder grains within the pattern. The reduction will evidently be most important for denser starting arrangements of powder particles, i.e., for a more packed powder. Moreover, as the reduction of grain velocities has greater effect in a more packed powder the saturation of the SL intensity at sufficiently high driving will be quickly achieved whereas more gradual saturation of the emission intensity is expected in a less packed powder. Closed and open circles in Fig. 5(b) apparently show such behaviors above points c. Finally, the validity of the proposed interpretation can be checked by analyzing the average SL intensity distributions presented by dashed curves in Figs. 3 and 4. It is readily seen that the SL intensity rapidly increases on ≈ 50 μm distance across the illuminating pattern in a more packed powder [panels (c) and (d) in Fig. 3] whereas much more gradual enhancement exhibited on ≈ 200 μm distance is observed in a less packed powder [panels (c) and (d) in Fig. 4]. This is likely due to viscosity movements of grains[17,18] across the axis of acoustic wave (in the x-axis direction in Figs. 3 and 4). These movements would lead to a rapid compaction of a more packed powder across the wave axis with a subsequent rapid enhancement in the emission intensity due to rapid decrease in ξ [see Eq. (1)]. The driven-induced grain movements in a less packed powder seem likely to be greater compared to that in a more packed powder thus explaining a gradual increase in the average SL intensity across the pattern seen in Figs. 4(c) and 4(d).

In addition, we test our model that connects the above observations with the interplay between particle velocities v and interparticle spacings ξ using the time evolution of the SL intensities after the drive is suddenly switched on or switched off. The relaxation after the drive is off always showed a rapid decay with a time constant shorter than the response time of our setup. When the drive is on rather complicated time evolutions were observed. In this measurement, data were collected for luminescence intensity versus the time after imposed driving, provided we allowed a powder to rest for a time interval t_0 after the previous driving cycle and then returned the driving voltage U to its original value above the luminescence threshold. In Fig. 7, the individual $I(t)$ curves are shown at different t_0 intervals, t being the time variable. Note that these measurements are not of steady-state powder packing densities as they follow the emission response to a rapid increase in the driving voltage amplitude. We see that, if the drive is switched off for

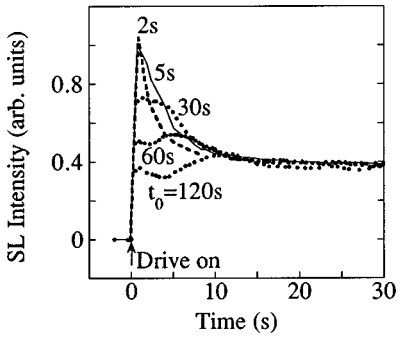

FIG. 7. Kinetics of SL taken in a more packed powder for five different values of time intervals t_0 between successive applications of the driving. Applied voltage $U=58$ V.

shorter than about 60 s ($t_0=2$, 5, and 30 s in Fig. 7), an enhanced SL intensity is observed just after the drive is on. If we allowed the powder to stay at rest for longer than about 120 s, the emission response after imposed driving behaves similar to $t_0=120$ s curve in Fig. 7. The imposed driving eventually results, to within experimental uncertainty, in the same emission intensity after approximately 10 s for different t_0.

In the framework of the presented model, v jumps dramatically as the drive is switched on. At this moment the SL intensity would rapidly increase as observed in Fig. 7. Then, as the drive is switched off v drops and the emission stops. Another feature of SL in powders is the effect of intergrain separations ξ on SL intensity. In order to investigate the relaxation of ξ in a more controlled way, we employed the evolution of the SL cross section. As shown in Fig. 8, the main effect is that the dense powder patterns relax only gradually with time. Indeed, the SL intensity distribution exhibited in Fig. 8(a) apparently shows more rapid increase in the intensity across the pattern compared to that presented in Fig. 8(b). This implies that the powder kept at rest for $t_0=2$ s likely retain dense particle patterns, but so far as we can determine by our technique, substantially looser packing of particles is observed at $t_0=120$ s. Therefore, the merging

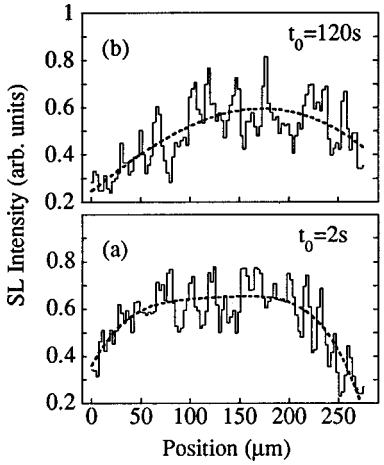

FIG. 8. Evolution of the SL intensity cross section in a more packed powder for two different values of time intervals t_0 between successive applications of the driving. The SL images were acquired over 1 s within 5 s after the application of the driving. Applied voltage $U=58$ V.

of dense patterns after the drive is off must be on time scales of a few minutes. Consequently, retained packing densities likely cause an enhancement in the SL intensity at a given driving voltage for a powder pre-exposed to acoustic driving (crosses in Fig. 5) compared to that taken in a freshly packed powder (closed circles in Fig. 5).

The competition between particle velocities subject to a rapid increase in the driving voltage and the retained particle packing drives the enhancement in the SL intensity at short instants in time after the drive is on (cf. at $t<10$ s in Fig. 7). The shorter the interval t_0 the more intense SL is observed at early times which is reasonably consistent with the fact that the shorter t_0 the greater retained density [i.e., the smaller ξ in Eq. (1)] is achieved. It appears anomalous, however, that the imposed driving can generate high-intensity emissions just after the drive is on at t_0 shorter than about 30 s. We suggest the following as a possible explanation. Once a powder is driven above point b in Fig. 5(b), and powder compaction occurs, reducing the driving voltage to zero initiates the powder density relaxation to a stable static state. When one starts the driving cycle again, a step increase in the drive pressure occurs that allows larger particle velocities than does a steady-state sinusoidal driving. We therefore believe that the transient behavior is captured during and after the driving voltage increase thus providing enhanced velocities at a given packing density retained from a previous run. This leads to the enhanced emission intensity in a nonrelaxed powder just after the drive is on in Fig. 7 which is eventually smoothed out to a steady-state value.

IV. CONCLUSIONS

In summary, we have demonstrated the use of sonoluminescence technique as a way to gain invaluable insights into particle agglomeration patterns in vibrating powders. The method enables direct studying of particle packing effects on the surface of a powder by imaging the evolutions of arbitrary cross sections of SL. In this way, the size of the patterns has been determined to be on the order of 10^2 μm in a 3-μm-sized powder of ZnS particles vibrating at a frequency of about 4 MHz. In addition, we have found the dependencies of the surface-integrated SL intensity on the driving voltage which are reasonably consistent with a simple molecular kinetic model of particle motions. It has been suggested that the SL technique can be used to obtain quantitative information about powder packing such as packing densities, density gradients, and particle velocity distributions within agglomeration patterns, relaxation times of dense powder arrangements.

ACKNOWLEDGMENTS

The work was supported by the Ministry of Education, Science, and Culture of Japan. We wish to thank Shozo Suto and Wakio Uchida for their help in the metal electrode deposition.

[1] For a review see H. M. Jaeger, S. R. Nagel, and R. P. Behringer, Rev. Mod. Phys. **68**, 1259 (1996).
[2] J. A. C. Gallas, H. J. Herrmann, and S. Sokolowski, Phys. Rev. Lett. **69**, 1371 (1992).
[3] K. Liffman, G. Metcalfe, and P. Cleary, Phys. Rev. Lett. **79**, 4574 (1997).
[4] K. Choo, T. C. A. Molteno, and S. W. Morris, Phys. Rev. Lett. **79**, 2975 (1997).
[5] A. Kudrolli, M. Wolpert, and J. P. Gollub, Phys. Rev. Lett. **78**, 1383 (1997).
[6] P. K. Haff, J. Fluid Mech. **134**, 401 (1983).
[7] J. T. Jenkins and S. B. Savage, J. Fluid Mech. **130**, 187 (1983).
[8] S. B. Savage, J. Fluid Mech. **194**, 457 (1988).
[9] G. W. Baxter, R. P. Behringer, T. Fagert, and G. A. Johnson, Phys. Rev. Lett. **62**, 2825 (1989).
[10] W. Wagner, R. S. Averback, H. Hahn, W. Petry, and A. Wiedenmann, J. Mater. Res. **6**, 2193 (1991).
[11] M. Nakagawa, S. A. Altobelli, A. Caprihan, E. Fukushima, and E.-K. Jeong, Exp. Fluids **16**, 54 (1993).
[12] V. Yu. Kuperman, E. E. Ehrichs, H. M. Jaeger, and G. S. Kraczmar, Rev. Sci. Instrum. **66**, 4350 (1995).
[13] G. E. Fasching and N. S. Smith, Jr., Rev. Sci. Instrum. **62**, 2243 (1991).
[14] S. Nasuno, A. Kudrolli, and J. P. Gollub, Phys. Rev. Lett. **79**, 949 (1997).
[15] O. A. Korotchenkov and T. Goto, Phys. Rev. B **56**, 13646 (1997).
[16] For a general review, see I. A. Viktorov, *Rayleigh and Lamb Waves* (Plenum, New York, 1967).
[17] W. L. M. Nyborg, in *Physical Acoustics*, edited by W. P. Mason (Academic, New York, 1965), Vol. 2B, p. 265.
[18] R. M. Moroney, R. M. White, and R. T. Howe, Appl. Phys. Lett. **59**, 774 (1991).